

z_1 oscillations in the stopping powers of silicon and tungsten for low-velocity channelled heavy ions

This article has been downloaded from IOPscience. Please scroll down to see the full text article.

1993 J. Phys.: Condens. Matter 5 3163

(<http://iopscience.iop.org/0953-8984/5/19/014>)

View [the table of contents for this issue](#), or go to the [journal homepage](#) for more

Download details:

IP Address: 171.66.16.159

The article was downloaded on 12/05/2010 at 14:00

Please note that [terms and conditions apply](#).

z_1 oscillations in the stopping powers of silicon and tungsten for low-velocity channelled heavy ions

V Hari Kumar and A P Pathak

School of Physics, University of Hyderabad, Hyderabad-500 134, India

Received 28 August 1992, in final form 30 November 1992

Abstract. A model of stopping for low-velocity heavy ions moving through an electron gas incorporating a shell model charge density has been used to calculate the stopping powers of silicon and tungsten for ions channelled along silicon (110) and tungsten (100) single crystals. The energy loss of the heavy ions is attributed to the scattering of target electrons in the potential field of a moving projectile. So the stopping cross section is proportional to the momentum transfer (or transport) cross section. A comparison of the results with experimental data and earlier theoretical calculation shows good agreement. The present model is most suited to projectile velocities greater than the Fermi velocity of target electrons.

1. Introduction

The stopping powers of solids for low-velocity channelled heavy ions exhibit a periodic (oscillatory) dependence on the charge z_1 of the incident channelled ions. This is referred to as z_1 oscillations [1, 2]. In this velocity region (i.e. of the order of $v_0 z_1^{2/3}$, where v_0 is the Bohr velocity), the nuclear stopping is small compared with electronic stopping and is further suppressed because close collisions of incident ions with target atoms are completely avoided in channelling. The maxima of electronic stopping occur (irrespective of whether it is the channelling or the random case and irrespective of the specific target medium) at around $z_1 = 6, 20, 38$ and minima occur at around $z_1 = 10, 29, 47$ [2]. In the channelling case the maximum-to-minimum ratio becomes large (as expected) and, when the velocity of the incoming projectile increases to above 3 au, the oscillations gradually damp out and ultimately disappear. The position dependence of stopping power in planar [3] and axial channels [4] has been calculated recently using shell charge densities and their planar and axial averages, showing good agreement with experimental results [3, 4]. This motivated us to use the shell model axial charge density to calculate z_1 oscillations in the channelling stopping-power case. One of us had been involved in work on stopping-power oscillations earlier [1, 5, 6]. In those papers, the effective charge density of target electrons was taken as the overlap of a moving projectile and an individual target atom or ion sited along the channel axis. Here we use the continuum average of atomic shell charge densities due to all the atoms along the relevant axis, also taking into account the appropriate geometry of the channel. This is in the spirit of the standard continuum model potential of channelling.

In section 2 we give a brief introduction of the shell model axial charge density. In section 3 the theory of the stopping power is outlined and the results are discussed in the concluding section, section 4.

2. Shell model axial charge density

Using one-term Slater orbitals with an optimized exponent given by Clementi and co-workers [7, 8], the spherically symmetric electron density due to one atom at a distance R from the centre is given by [4]

$$\rho(R) = \frac{1}{4\pi R^2} \sum_j \omega_j R^2 N_j^2 R_j^2 \quad (1)$$

where ω_j is the occupation number of the j th shell, R_j is the corresponding radial wavefunction with normalization N_j given by

$$N_j = (2\xi_j)^{n_j+1/2} / [(2n_j)!]^{1/2} \quad (2)$$

where n_j is the principal quantum number and ξ_j is the corresponding orbital exponent.

The axial charge density due to one string is calculated using the continuum approximation [4] and is given by

$$\rho_A(r) = \frac{1}{d} \int_{-\infty}^{\infty} \rho(\sqrt{r^2 + z^2}) dz \quad (3)$$

The local electron density at a distance r from the axis is

$$\rho_A(r) = \frac{1}{\pi d} \sum_j \frac{\omega_j}{(2n_j)!} \sum_{m=0}^{n_j-1} \frac{2^{2m} (2(n_j - m))! (n_j - 1) \xi_j^{n_j+m+2} r^{n_j+m} K_{n_j-m}(2\xi_j r)}{(n_j - m - \frac{1}{2})(n_j - m)(m)! [(n_j - m - 1)!]^2} \quad (4)$$

where d is the interatomic spacing and K_{n_j-m} the modified Bessel function.

In the silicon case, a $\langle 110 \rangle$ axial channel is nearly symmetric and we approximate that the six rows form a regular hexagon. In the $\langle 100 \rangle$ channel of tungsten, the four rows form a square. The charge density due to all the strings (six for silicon $\langle 110 \rangle$ and four for tungsten $\langle 100 \rangle$) is calculated as a function of distance measured from the channel axis.

3. Electronic stopping power

The z_1 oscillations in the stopping power were theoretically explained by modifying the Firsov theory [1] and, even though these modified theories predict the positions of the maxima and minima correctly, these theories fail to explain the large value of the maximum-to-minimum ratio of stopping power shown in experiments. Damping of the z_1 oscillations at higher z_1 -values is another shortcoming of these theories. Our calculations are based on the semiclassical theory proposed by Briggs and Pathak [1]. In this theory, energy loss is attributed to the scattering of target electrons in the potential field of the moving projectile. At these low velocities, most of the stopping-power contribution comes from a transfer of momentum between the electrons of the ion and those of the target atom because of overlap of electronic clouds as the ion passes. This transfer of momentum can be considered to be affected by the elastic scattering of the target electrons through the charge cloud of the moving ion. This is similar to the diffusion of electrons through gases.

The mean energy lost per unit path length by an ion with velocity v has been shown to be

$$-dE/dx = nmv^2 Q_d \quad (5)$$

where m is the electron mass, n is the density of electrons and Q_d is the momentum transfer cross section (transport cross section) and has been shown to be

$$Q_d = 2\pi \int_0^\pi I_0(\theta)(1 - \cos \theta) \sin \theta \, d\theta \tag{6}$$

where $I_0(\theta)$ is the elastic scattering intensity. The momentum transfer cross section can be written [9] as

$$Q_d = \frac{4\pi}{k^2} \sum_l (l + 1) \sin^2(\eta_l - \eta_{l+1}) \tag{7}$$

where $\hbar k$ is the electron momentum in the centre-of-mass frame. The phase shift η_l of the l th partial wave of the electron wavefunction can be calculated by numerically solving the radial part of the Schrödinger equation:

$$d^2G_l/dr^2 + [k^2 + U(r) - l(l + 1)/r^2]G_l = 0 \tag{8}$$

where G_l is the radial wavefunction corresponding to the l th partial wave and k is the electron wavenumber corresponding to the projectile velocity and $U(r) = (2m/\hbar^2)V(r)$ where $V(r)$ represents interaction between target electron and projectile.

Since the potential between the electron and projectile $V(r)$ varies more rapidly than $1/r$, the asymptotic form of the radial wavefunction can be written as

$$G_l(r) \sim \sin(kr - \frac{1}{2}l\pi + \eta_l). \tag{9}$$

In the absence of an atomic field, equation (8) gives the solution whose asymptotic form is

$$G_l(r) \sim \sin(kr - \frac{1}{2}l\pi). \tag{10}$$

The magnitude of the phase shift η_l is determined by the competition between the attractive potential $U(r)$ and the repulsive centrifugal potential $l(l + 1)/r^2$ and is computed by finding the shift in the nodes of solution (9) with respect to the corresponding node of the solution (10) for large r . The atomic field $U(r)$ in which the target electrons are scattered is taken to be the Molière potential (in the Thomas–Fermi statistical model). The above model had been proposed and successfully used to explain not only the z_1 oscillation and the z_2 variation [10], but also the velocity dependence of these oscillations [11]. Some alternative models [12–16] have been proposed in recent years. These are mostly very detailed density-functional theory calculations [17, 18] for $V(r)$ which also yield information on the effective charge density used in stopping-power formulae. The agreement with experimental results is approximately of the same order as our results. Moreover the velocity dependence of the z_1 oscillation in these models has not yet been calculated to show at which projectile velocity the oscillations should vanish. Calculation of the transport cross section at the Fermi velocity as done in these later models is valid only for a degenerate electron gas in metals but certainly not for semiconductors such as Ge or Si or orbital target electrons such as 5d or 4d. Consequently we have made our calculations for *projectile velocities* as earlier [1] because of reasonable agreement with experimental results and analytical applicability to more complicated situations involving defects.

The charge density n was calculated [1, 5] for individual target atoms along the particular channel. Here the charge density n in equation (5) is calculated as illustrated in section 2. The shell axial charge density (equation (4)) is curve fitted to a simple exponential function of the form $\rho_A(r) = ae^{br^2} + c$, where parameters a , b and c are given

by $a = 0.00433592$, $b = 0.4154959$ and $c = 0.0122899$ for tungsten (100) and by $a = 0.000154$, $b = 0.72756310$ and $c = 0.01221266$ for silicon (110). Atomic units are used here and also in what follows. The effective charge density n_{eff} is calculated by integrating over the space occupied by the projectile ion:

$$n_{\text{eff}} = \frac{1}{\pi R_s^2} \int_0^{R_s} 2\pi r \rho_A(r) dr \quad (11)$$

where R_s is the relevant space occupied by the moving ion and is taken as the radius of the maximum charge density [19] of the outermost shell of the projectile ion appropriate to the most probable charge state. For example projectiles such as rare gases are assumed to be neutral whereas those of alkali-metal ions (Na, K, etc) are assumed to be singly charged because their outermost s electrons will certainly be stripped off during their motion in solids. In equation (11), r is measured from the centre of the channel. In the case of tungsten, we considered the conduction $6s$ electrons to contribute a uniform electron gas so that n_{6s} for tungsten is twice the atomic density. The axial charge density is calculated only for shell electrons (i.e. up to $5d$ electrons), i.e.

$$n(r) = n_{\text{eff}}(r) + n_{6s} \quad (12a)$$

for the tungsten case and

$$n(r) = n_{\text{eff}}(r) \quad (12b)$$

for the silicon case.

In atomic units, equation (5) changes to

$$-dE/dx = 4\pi n \bar{Q}_d \quad (13)$$

where $\bar{Q}_d = \sum_l (l+1) \sin^2(\eta_l - \eta_{l+1})$.

The stopping power is calculated using equation (13) for various channelling projectile ions at a velocity of 0.75 au for both silicon and tungsten target atoms. This is shown in figure 1 (silicon (110)) and figure 2 (tungsten (100)), respectively.

4. Conclusion

We have calculated the stopping power of silicon (along the (110) axis) and tungsten (along the (100) axis) for low-velocity channelled heavy ions and compared the results with earlier theoretical calculations and experimental results. This is shown in figures 1 and 2, respectively. The main aim of this work has been to keep the problem analytical as far as possible so that applications to the effects of defects and disorder [20, 21] on this important quantity can be easily estimated. Of course, more detailed calculations using non-linear density-functional formalism [17, 18] have been performed which also yield z_1 oscillations [13, 14]. In these calculations, even after excessive computational efforts were made for potential and charge-density calculations, the effective electron density sampled in channelled particles is determined by equating the theoretical and experimental values of stopping for some specified z_1 (e.g. for silicon (110) a z_1 -value of 5 was chosen to implement the fitting [13]). These calculations are ideally suited to a degenerate electron gas in the limit when the projectile velocity is negligibly small compared with the Fermi velocity so that the projectile velocity dependence of oscillations does not appear in the problem. Our calculations are valid for projectile velocities greater than the target electron

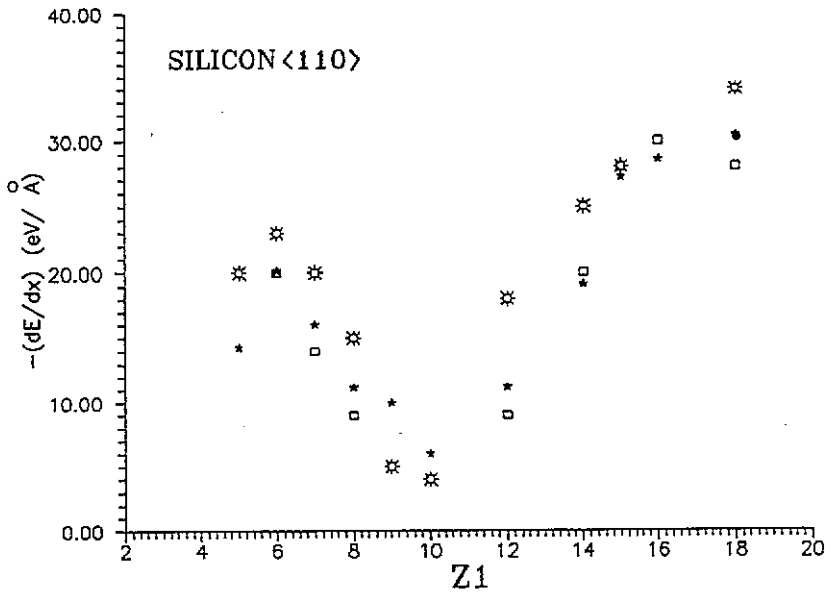


Figure 1. The stopping power of silicon for heavy ions channelled along the $\langle 110 \rangle$ axis at a projectile velocity of $1.5 \times 10^8 \text{ cm s}^{-1}$: open star, experiment of Eisen [22]; \square , calculation of Briggs and Pathak [5]; \star , calculation using the shell model charge density.

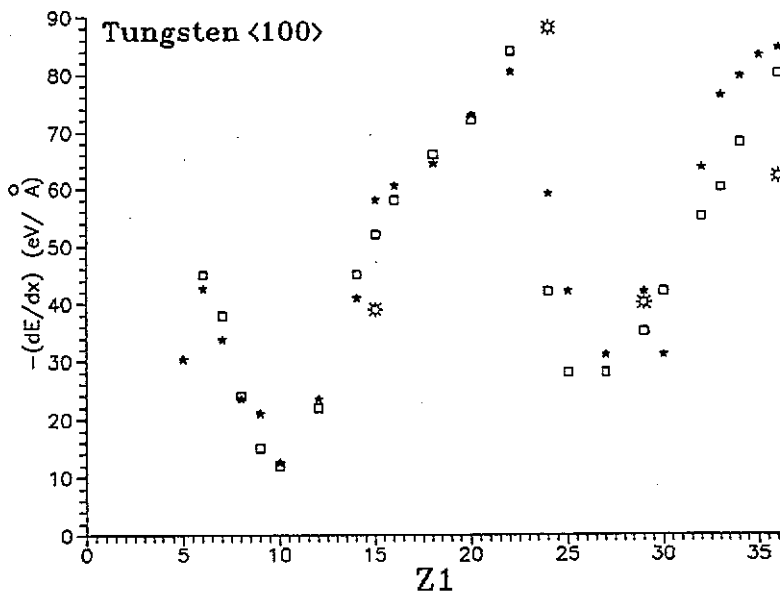


Figure 2. Stopping power of tungsten for heavy ions channelled along the $\langle 100 \rangle$ direction at a projectile velocity of $1.5 \times 10^8 \text{ cm s}^{-1}$: open star, experiment of Eriksson *et al* [23]; \square , calculation of Pathak [6]; \star , calculation using the shell model charge density.

velocities (i.e. when the Fermi velocity as well as the outer orbital electrons contribute to the stopping of well channelled projectiles). *In fact all the experimental data available to date are in this velocity range ($v > v_F$).*

As discussed earlier [1–6], we assumed elastic scattering of free (loosely bound) electrons from the well channelled projectiles. The actual shell electron density is averaged along the channel in an appropriate geometry, and the appropriate size effect of the projectile is included. There is no scaling or best fitting done as far as the final stopping power is concerned. The conduction electrons (such as 6s in tungsten) are assumed to contribute entirely as before [6]. Apparent disagreement for some values of z_1 (e.g. $z_1 = 24$) is actually related to a shift in the phase of the oscillations, with changes in the relative velocity [11]. The validity of the approximation of taking the projectile velocity as the relative velocity increases as v increases.

Overall, our calculations, in spite of being simplistic, are reasonably accurate and useful. We feel that the data for heavy projectile ions ($z_1 > 30$) are very sparse and further experiments are needed to study these oscillations for heavier ions. Moreover, a systematic experimental study with respect to velocity dependence has never been undertaken, even though it is known that, at high velocities beyond the maximum in the stopping power versus velocity curve, the oscillations do not exist. Such interesting experiments are strongly suggested.

Acknowledgment

This work was supported by the Department of Science and Technology, New Delhi, India, through a research project.

References

- [1] Briggs J S and Pathak A P 1973 *J. Phys. C: Solid State Phys.* **6** L153, and references therein
- [2] Pathak A P 1982 *Radiat. Eff.* **61** 1, and references therein
- [3] Pathak A P 1978 *Phys. Status Solidi b* **86** 751
- [4] Agnihotri R and Pathak A P 1992 *Nucl. Instrum. Methods B* **67** 39
- [5] Briggs J S and Pathak A P 1974 *J. Phys. C: Solid State Phys.* **7** 1929
- [6] Pathak A P 1974 *J. Phys. F: Met. Phys.* **4** 1883
- [7] Clementi E and Raimondi D L 1963 *J. Chem. Phys.* **38** 2686
- [8] Clementi E, Raimondi D L and Reinhardt W P 1967 *J. Chem. Phys.* **47** 1300
- [9] Massey H S W and Burhop E M S 1969 *Electronic and Ionic Impact Phenomena* vol 1 (Oxford: Clarendon)
- [10] Pathak A P 1974 *J. Phys. C: Solid State Phys.* **7** 3239
- [11] Pathak A P 1980 *Phys. Rev. B* **22** 96 and 5544
- [12] Puska M J and Nieminen R M 1983 *Phys. Rev. B* **27** 6121
- [13] Echenique P M, Nieminen R M, Ashley J C and Ritchie R H 1986 *Phys. Rev. A* **33** 897
- [14] Penalba M, Arnau A and Echenique P M 1992 *Nucl. Instrum. Methods B* **67** 66
- [15] Ferrell T L and Ritchie R H 1977 *Phys. Rev. B* **16** 115
- [16] Wang Y N, Ma T C and Gong Y 1992 *Phys. Lett.* **167A** 287
- [17] Hohenberg P and Kohn W 1964 *Phys. Rev. B* **136** 864
- [18] Kohn W and Sham L J 1965 *Phys. Rev. A* **140** 1133
- [19] Slater J C 1960 *Quantum Theory of Atomic Structure (i)* (New York: McGraw-Hill) p 210
- [20] Pathak A P 1977 *Phys. Rev. B* **15** 3309
- [21] Pathak A P and Balagari P K J 1986 *Appl. Phys. Lett.* **48** 1075
- [22] Eisen F H 1968 *Can. J. Phys.* **46** 561
- [23] Eriksson L, Davies J A and Jespersgaard P 1967 *Phys. Rev.* **161** 219